

A one-pot hydrothermal synthesis of tunable dual heteroatom-doped carbon microspheres

Electronic Supplementary Information

Stephanie-Angelika Wohlgemuth,^{a,*} Filipe Vilela,^a Maria-Magdalena Titirici^a and Markus Antonietti^a

^a Max Planck Institute of Colloids and Interfaces, Am Mühlenberg 1, 14467 Potsdam, Germany. Fax: +4-331-56- 9502; Tel: +49-331-567-9562; E-mail:

stephanie.wohlgemuth@mpikg.mpg.de

Sample characterization

SEM images were recorded on a LEO 1550/LEO GmbH Oberkochen provided with an Everhard Thornley secondary electron and in – lens detectors. **XRD** patterns were recorded on a Bruker D8 diffractometer over the 2θ range of 5 to 80° using Cuα radiation and a scan rate of 1 ° min⁻¹. **Thermogravimetric analysis** was carried out using a NETZSCH TG 209 from 0 °C to 1000 °C at a heating rate of 10 Kmin⁻¹ under N₂. **¹³C solid state MAS NMR** spectra were acquired on a Bruker Avance 300 MHz (7T) spectrometer using 4mm zirconia rotors as sample holders, spinning at MAS rate of 14 kHz. The chemical shift reference was tetramethylsilane (TMS). 1H t1 relaxation time was set to 3 s. Proton-to-carbon CP MAS was used to enhance carbon sensitivity with a cross polarization time equal to 1 ms. **Gas Sorption Analysis** for the determination of carbon surface areas and pore size distributions were measured by nitrogen adsorption and desorption at 77.3 K using Autosorb 1MP or Quadrasorb Kr/MP machines (Quantachrome Instruments). Carbon dioxide sorption isotherms were collected at 273 K using the same device. High purity gases were used. Data evaluation was performed using the AS1Win Software from Quantachrome Instruments. Pore size distributions and pore volumes were derived from the adsorption branches of the isotherms using the Brunauer-Emmet-Teller (BET) model (N₂, assuming carbon adsorbent with slit pores) or the Non-linear density functional theory (NLDFT) method (CO₂, assuming carbon adsorbent with slit pores). Samples were degassed at 150 °C for 20 h under high vacuum before analysis. **Elemental Analysis** was carried out using a Vario MICRO Cube analyzer from Elementar Analysensysteme GmbH. **XPS analysis** of the samples was performed using a Thermo Scientific Kα ESCA instrument equipped with Al Kα_{1,2} monochromatized radiation at 1486.6 eV X-ray source. Charge neutralization was performed by using both a low energy flood gun (0 to 14 eV) and a low energy Ar ion gun. The XPS measurements were carried out using monochromatic Al-Kα radiation (hν = 1486.6 eV). Photoelectrons were collected at 90° to the sample surface. A constant analyzer energy mode (CAE) with 100 eV pass energy for survey spectra and 20 eV pass energy for high resolution spectra was used. The spectra were calibrated by setting the C1s photo peak at 285.0 eV. For sulfur, the S2p_{3/2} peak was used for the assignment of binding states. **Specific conductivity** measurements were carried out with Gamry Reference 600/3000 potentiostat (Gamry Instruments) and Gamry EIS 300/Physical Electrochemistry software. Electrical conductivity was achieved applying R-model on potentiostatic impedance spectroscopy at 1-1000 Hz using a two electrode setup.

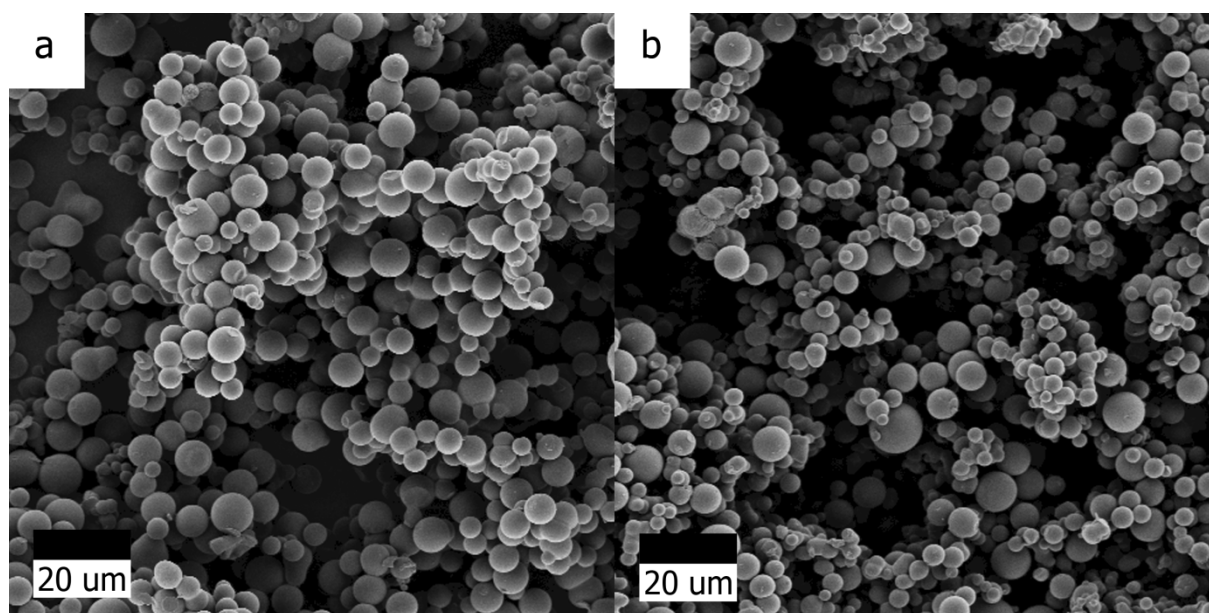


Fig. S1 SEM images of pyrolyzed HTC products of a) glucose with cysteine (Cys0.2_900) and b) glucose with thienyl-cysteine (TCys0.2_900). Pyrolysis does not seem to affect the particle morphology as compared to the as-synthesized samples Cys0.2 and TCys0.2 after HTC at 180 °C.

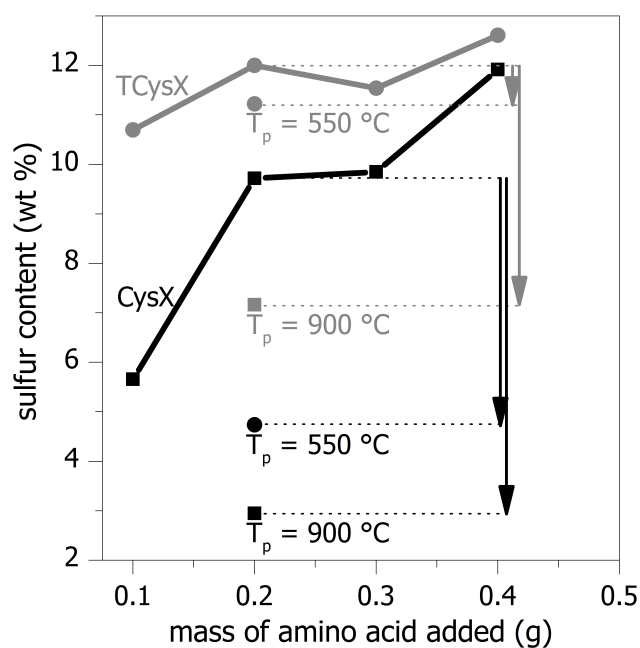


Fig. S2 A summary of the correlation of amount of amino acid addition with the final sulfur content. Data for the cysteine series is shown in black and data for the thienyl-cysteine series in grey. The single data points correspond to Cys0.2_550 and TCys0.2_550 (black and grey circle, respectively), and Cys0.2_900 and TCys0.2_900 (black and grey square, respectively). For CysX the sulfur content increases with increasing mass addition of cysteine and the sulfur loss upon pyrolysis is high. For TCysX, the sulfur content changes only slightly with varying mass addition of thienyl-cysteine, and hardly any sulfur loss is observed at $T_p = 550^\circ\text{C}$. At $T_p = 900^\circ\text{C}$, high levels of sulfur are retained, compared to Cys0.2_900.

Table S1 XPS peak assignments of the C 1(s) photoelectron envelopes for Cys0.2 and TCys0.2 after hydrothermal treatment at 180 °C and after pyrolysis at 550 °C and 900 °C.

Peak	Binding Energy (eV)						Assignment
	fraction of species (%)						
	Cys0.2	Cys0.2_550	Cys0.2_900	TCys0.2	TCys0.2_550	TCys0.2_900	
C1s	285	285	285	285	285	285	sp ² C-C or C-H ^{19, 22, 25}
	64.1	72.3	73.3	44.4	84.8	74.5	
	286.38	286	286.2	286.1	286.3	286	C-O / C-N / C-S ²²
	25.2	23.3	15.0	47.1	12.8	15.8	
	287.84	288.18	287.54	288.1	288.35	287.3	C=O / C=N ^{22, 37}
6.5	2.1	4.7	6.4	2.3	4.7		
289.08	289.6	289.04	289	-	289.03	O=C-O ³⁷	
4.2	2.3	3.8	2.1	-	3.6		
-	-	191.1	-	-	-	291	π - π^* shake up satellite ^{12, 25}
-	-	3.3	-	-	-	1.4	

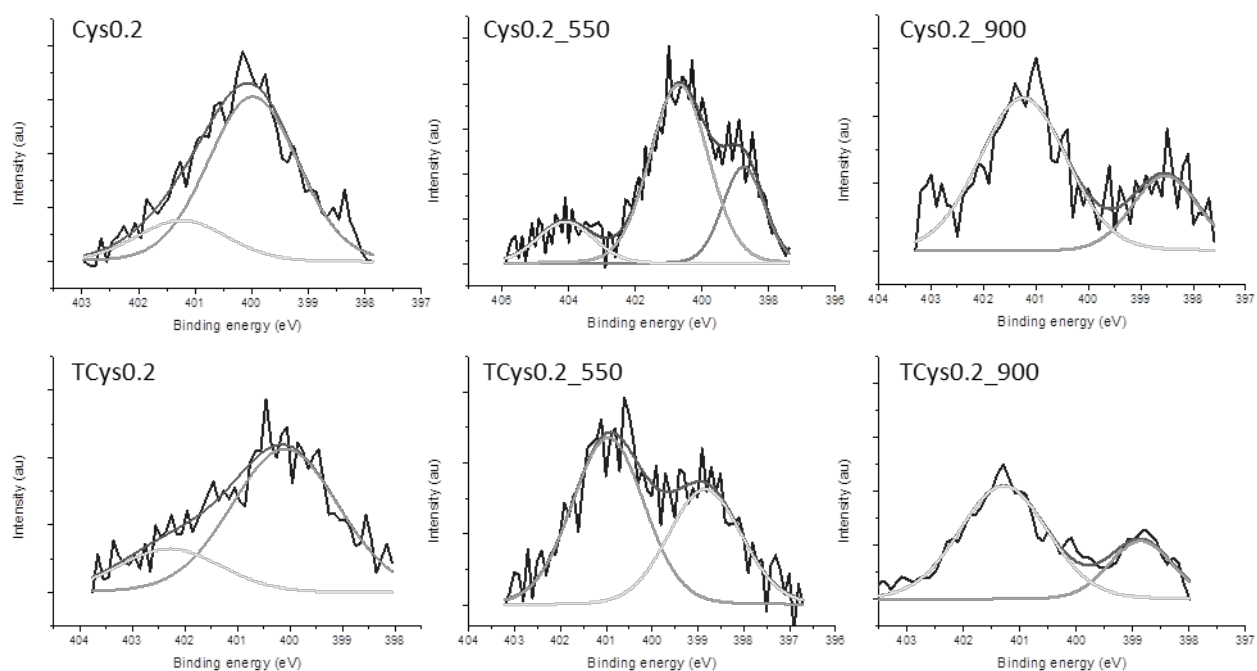


Fig. S3 Deconvoluted high resolution XPS of the N 1(s) photoelectron envelopes for Cys0.2 and TCys0.2 after hydrothermal treatment at 180 °C and after pyrolysis at 550 °C and 900 °C.

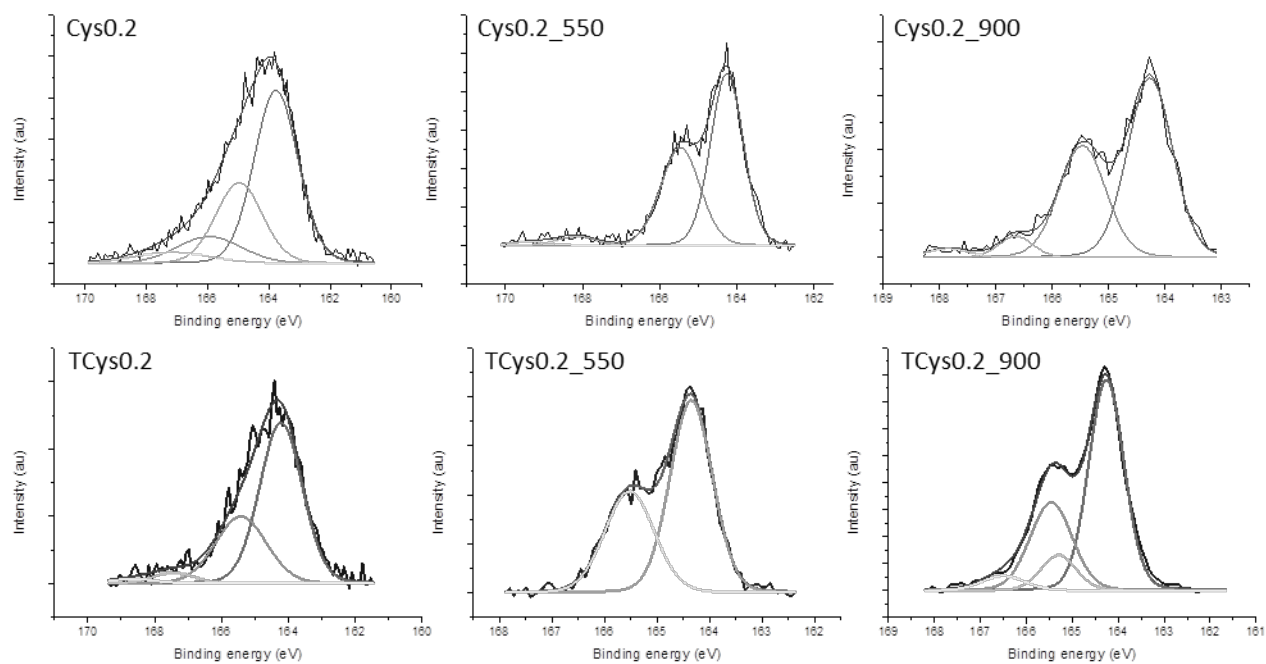


Fig. S4 Deconvoluted high resolution XPS of the S 2(p) photoelectron envelopes for Cys0.2 and TCys0.2 after hydrothermal treatment at 180 °C and after pyrolysis at 550 °C and 900 °C.